International Journal of Energy and Power Engineering
2014; 3(6-2): 27-37
Published online December 26, 2014 (http://www.sciencepublishinggroup.com/j/ijepe)
doi: 10.11648/j.ijepe.s.2014030602.15
ISSN: 2326-957X (Print); ISSN: 2326-960X (Online)

3-level H-bridge space vector PWM inverter for induction motor

Darshni Shukla[1], Brijal Panchal[2], Pragya Nema[3]

[1]Electrical Engg. Dept, Government engineering college, Valsad, India
[2]Electrical Engg. Dept, S V M Institute of Technology, Bharuch, India
[3]Electrical Engg. Dept, Lakshmi Narayan College of Technology, Indore, India

Email address:

darshnishukla@yahoo.com (D. Shukla), brijusvmit@gmail.com (B. Panchal), dr.pragyanema@gmail.com (P. Nema)

To cite this article:

Darshni Shukla, Brijal Panchal, Pragya Nema. 3-Level H-Bridge Space Vector PWM Inverter for Induction Motor. *International Journal of Energy and Power Engineering.* Special Issue: Distributed Energy Generation and Smart Grid. Vol. 3, No. 6-2, 2014, pp. 27-37.
doi: 10.11648/j.ijepe.s.2014030602.15

Abstract: Multilevel voltage-fed inverters with space vector pulse width modulation strategy are gained importance in high power high performance industrial drive application & better dc bus utilization. In the propose scheme 3-level space vector PWM H-bridge inverter has a large number of switching states as conventional 2-level VSI. A step by step & detail study is described here so it can be implemented to multi level inverter also. MATLAB/SIMULINK implementation & experimental results of SVPWM inverter & its FFT analysis are presented to realize the validity of the inverter operation in linear region.

Keywords: Space Vector PWM, 3-Level Inverter

1. Introduction

Large electric drives and utility applications require advanced power electronics converters to meet high power demand. As a result multilevel power converter structure has been introduced as an alternative in high power and medium voltage situation. Three level voltage-fed PWM inverters are recently showing popularity for multi-megawatt industrial drive application. The output voltage waveforms in multilevel inverter can be generated at low switching frequency with high efficiency and low distortion.

PWM techniques have been developed for inverter circuit to reduce the magnitude of the harmonics and to allow control of the fundamental component of output voltage. The advantage over two levels SVPWM is due to 27 switching states so redundancy is higher. This paper propose 3-level H-bridge SVPWM inverter, which is suitable for separate DC Source. Mathematical analysis, simulation and hardware results with separated DC sources have been performed with resistive load and induction motor.

2. Switching States for Space Vector PWM for Three Level H-Bridge Inverter

Switching states for three phase three level inverter = m^n, where m=number of levels and n=number of phases. Total 27 switching states can be utilized which are shown in Fig. 2. Out of them twenty four are active states and three are zero vectors which are lies on the centre of Hexagon [1].Table '1' shows the significance of switching states according to Fig. 1.

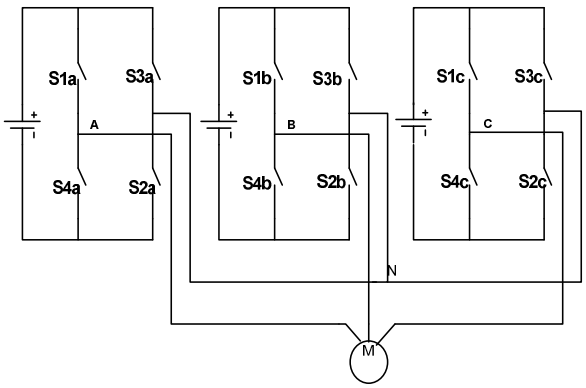

Figure 1. *Three phase H-bridge*

Table 1. *switching states table*

Switching States	Device switch status (a-phase unit)				Inverter Terminal voltage (Van)
	S1	S2	S3	S4	
1	on	on	off	off	+Vdc
	on	off	on	off	
0	or				0
	off	on	off	on	
-1	off	off	on	on	-Vdc

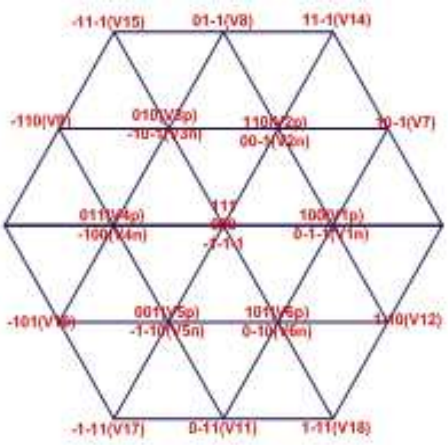

Figure 2. *Space vector switching diagram*

Entire space vector diagram is divided in six sectors and twenty four regions. Each sector consists of four regions. An instantaneous reference input vector may lie in any of these regions at any point of time [2]. Appendix A lists the projections of different switching vectors in α-β reference frame in terms of dc-link voltages.

3. Generation of Space Vectors Pulse Width Modulation

In the proposed method, the design steps are as follows (i) Clarke's transformation (ii) identification of sector (iii) identification of regions (iv) duty cycle calculations (v) PWM pulse generation and pulse assignment.

3.1. Clarke's Transformation

It is a mathematical transformation used to simplify the analysis of three phase circuits. Here it gives generation of reference signal used for space vector modulation control of three phase inverters.

$$V_\alpha + jV_\beta = \frac{2}{3}\left(V_a + e^{j\frac{2\pi}{3}}V_b + e^{-j\frac{2\pi}{3}}V_c\right) \tag{1}$$

$$V_\alpha + jV_\beta = \frac{2}{3}\left(V_a + \cos\frac{2\pi}{3}V_b + \cos\frac{2\pi}{3}V_c\right) + j\frac{2}{3}\left(\sin\frac{2\pi}{3}V_b - \sin\frac{2\pi}{3}V_c\right) \tag{2}$$

$$\begin{bmatrix} v_\alpha \\ v_\beta \end{bmatrix} = \frac{2}{3}\begin{bmatrix} 1 & \frac{-1}{2} & \frac{-1}{2} \\ 0 & \frac{\sqrt{3}}{2} & \frac{-\sqrt{3}}{2} \end{bmatrix}\begin{bmatrix} v_{an} \\ v_{bn} \\ v_{cn} \end{bmatrix} \tag{3}$$

3.2. Sector Identification Algorithm

Projections of command vector v on α-β axes are calculated and comparison between them is used to identify sector as shown in flowchart in Fig. 3.

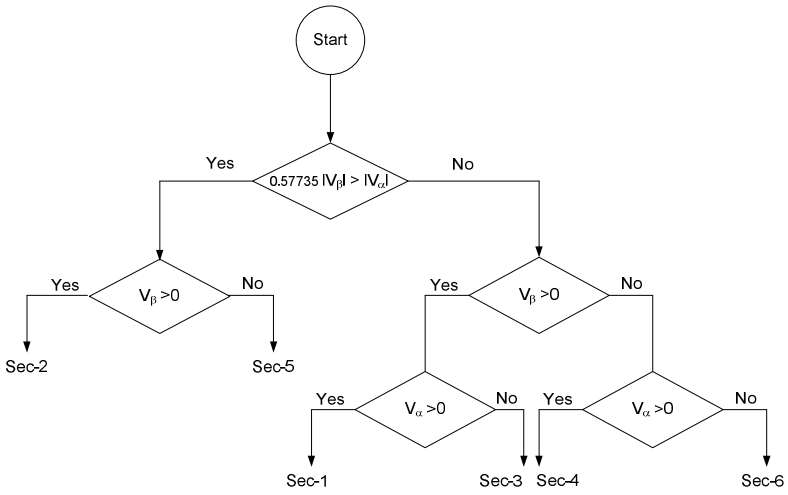

Figure 3. *Sector identification flowchart*

3.3. Region Identification Algorithm

Each sector is divided in equal four regions, so theta varies from zero to sixty degree in every sector. Value of m_1 & m_2 which will be derived from α&βaxes projections as shown in Fig. 4.and from this value flow chart has been developed as shown in Fig.5. Once sector & region is determined the switching sequence needs to be arranged so that ripple content in output current is minimum [6].

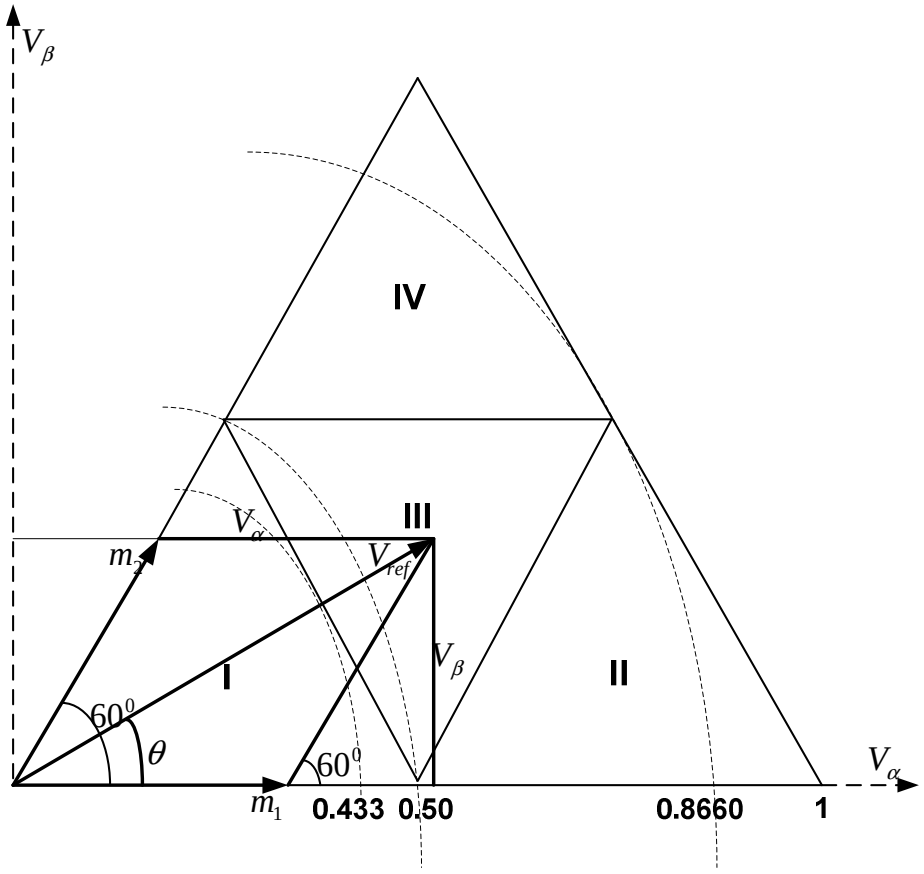

Figure 4. *Region separation in one sector*

$$\theta = 0:60$$

$$V_\alpha = V_{ref} * \cos\theta$$

$$V_\beta = V_{ref} * \sin\theta$$

$$\sin 60^0 = \frac{V_\beta}{m_2}$$

$$\therefore m_2 = \frac{2}{\sqrt{3}} * V_\beta .....(4)$$

$$\cos 60^0 = \frac{V_\alpha - m_1}{m_2}$$

$$\therefore \frac{1}{2} = \frac{V_\alpha - m_1}{m_2}$$

$$\therefore \frac{m_2}{2} = \frac{V_\alpha - m_1}{m_2}$$

$$\therefore m_1 = V_\alpha - \frac{m_2}{2}$$

$$\therefore m_1 = V_\alpha - \frac{V_\beta}{\sqrt{3}} ....(5)$$

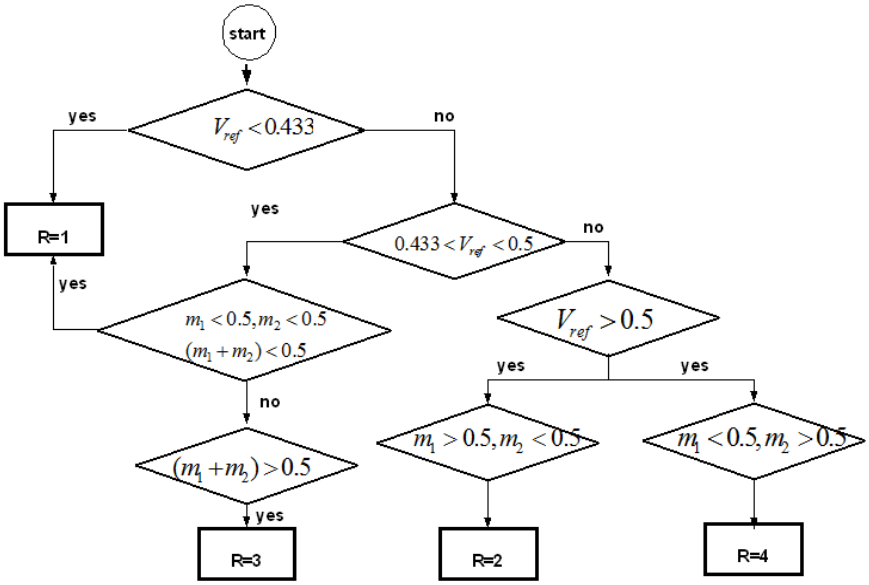

Figure 5. *Region identification flowchart*

3.4. Duty Ratio Calculation

In linear region, the rotating reference vector always remains within the hexagon. The largest output voltage magnitude is the largest radius of inscribed circle within the hexagon. This means that linear region ends when the reference voltage is equal to the radius of circle inscribed within the hexagon.

The time duration of switching vectors is computed in terms of duty cycle d_1, d_2 and d_3 corresponds to non-zero switching vectors & another duty cycle d_0 corresponds to zero or null vector. The combination of the duty cycle is based on calculation of geometric projection of the referencevector on α andβ axis which is shown in (Appendix A).

For region '1'of all the sector we can find 2X2 projection matrix and for regions'2', '3'and'4' 3 X 3 matrix will be required. So at any given instant duty cycle matrix D can be found fromInverse of projection matrix*[V_α ;V_β] and projection matrix*[V_α ;V_β;1] respectively.

If the reference vector lies in the inner hexagon, only two equations are sufficient to calculate d_1 & d_2. For e.g. If the vector is in sector '1'and region '1' the duty cycle is computed usingEq. (6)

$$\begin{bmatrix} d_1 \\ d_2 \end{bmatrix} = \frac{1}{K} \begin{bmatrix} \frac{1}{2} & \frac{1}{4} \\ 0 & \frac{\sqrt{3}}{4} \end{bmatrix}^{-1} \begin{bmatrix} V_\alpha^* \\ V_\beta^* \end{bmatrix} \qquad (6)$$

Where, $K=\frac{2}{3}V_{dc}$, $d_0 = 1-(d_1+d_2)$, (only for region one).

If the reference vector lies in the outer hexagon the vector to be switched are all non-zero active vector. Therefore to solve the duty cycle matrix $\begin{bmatrix} d_1 \\ d_2 \\ d_3 \end{bmatrix}$ three equations are required. We can use $d_1+d_2+d_3=1$ as the third equation. For e.g. If the reference vector lies in sector'1' and region '2', the vectors to be switched are V_{13},V_7 and V_1.The duty cycle is computed using Eq. (7)

$$\begin{bmatrix} d_1 \\ d_2 \\ d_3 \end{bmatrix} = \begin{bmatrix} \left(\frac{2}{3}v_{dc}\right) & \frac{3}{4}\left(\frac{2}{3}v_{dc}\right) & \frac{1}{2}\left(\frac{2}{3}v_{dc}\right) \\ 0 & \frac{\sqrt{3}}{4}\left(\frac{2}{3}v_{dc}\right) & 0 \\ 1 & 1 & 1 \end{bmatrix}^{-1} \begin{bmatrix} v_\alpha \\ v_\beta \\ 1 \end{bmatrix} \qquad (7)$$

3.5. Pulse Generation & Assignment

It has been assumed that the duty-cycle values are already known prior to this step.The PWM waveforms are generated by comparing the three signals with a triangular waveform of constant switching frequency equals to the sampling frequency of the modulator [7].For an e.g. the generation of PWM waveforms for sector '1' region '4' is explained with the help of Fig. 6.

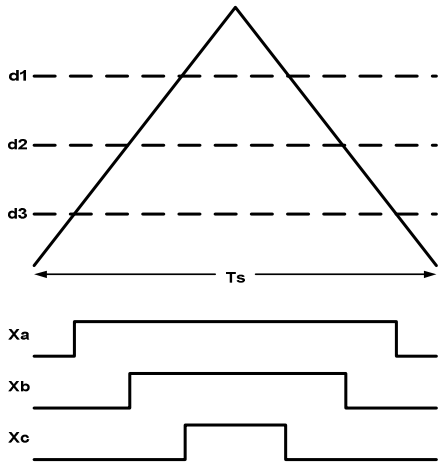

Figure 6. *Principle of PWM waveform generation*

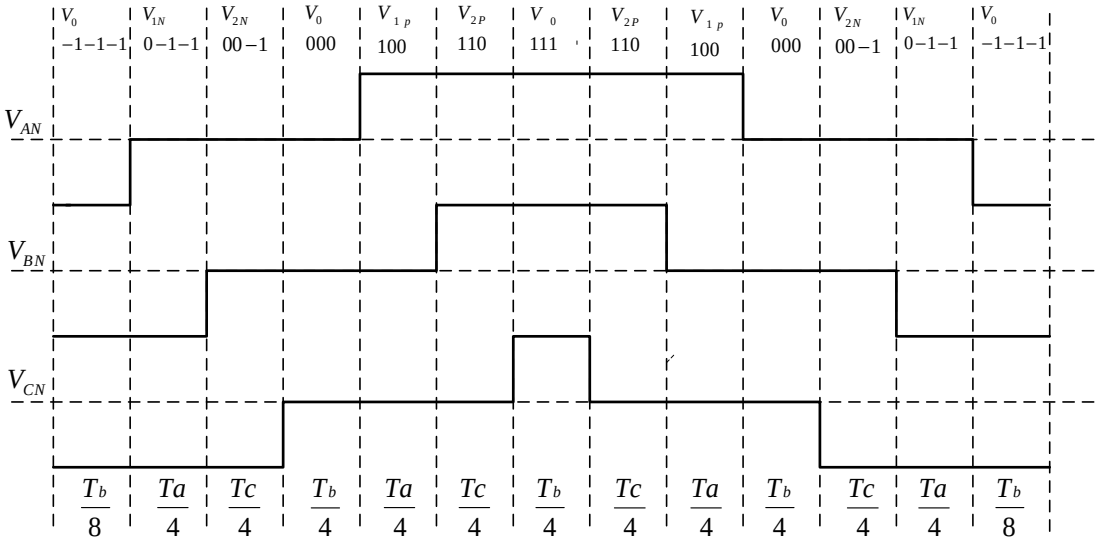

Figure 7. *Region 1 pulse pattern*

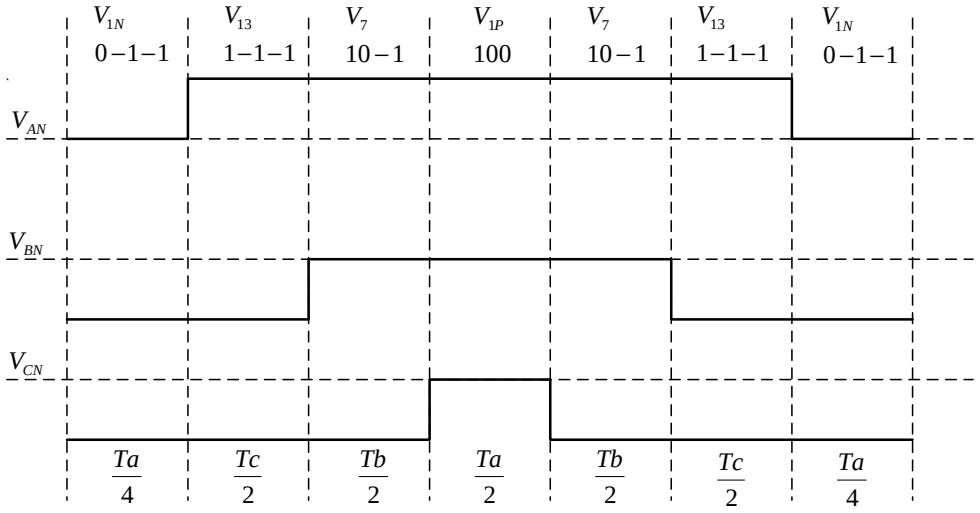

Figure 8. *Region 2 pulse pattern*

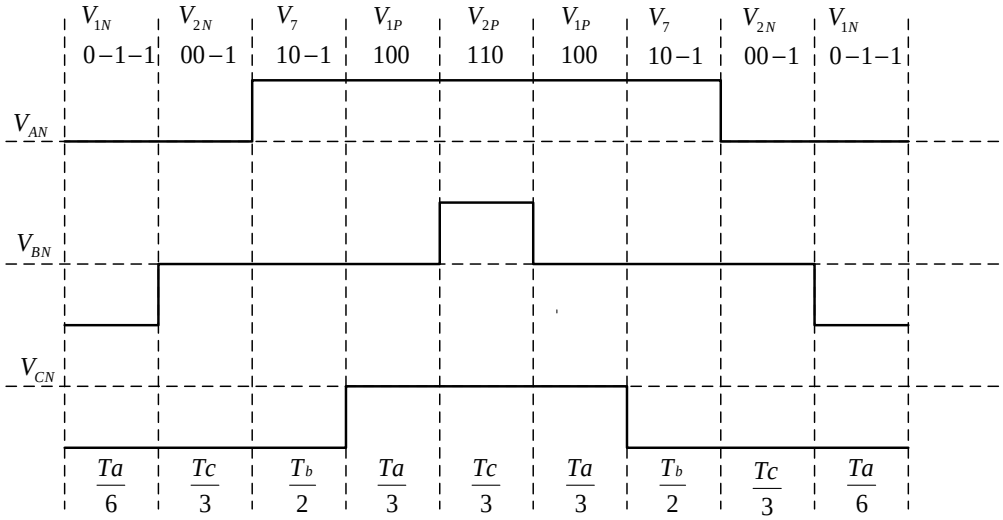

Figure 9. *Region 3 pulse pattern*

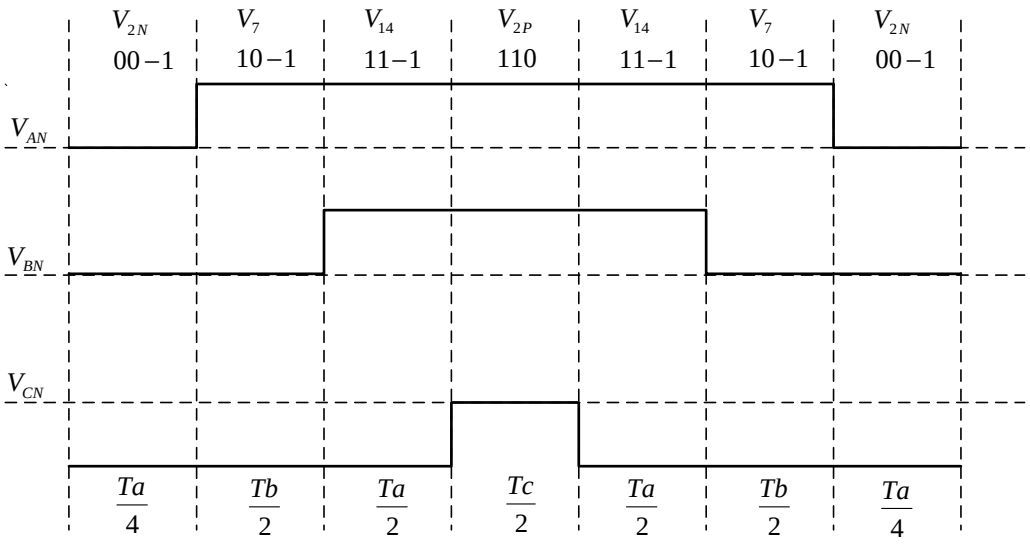

Figure 10. *Region 4 pulse pattern*

Table 2. *Sector wise switching pulse assignment*

S=1	S=2	S=3	S=4	S=5	S=6
x_a	x_b	x_c	x_c	x_b	x_a
x_b	x_a	x_a	x_b	x_c	x_c
x_c	x_c	x_b	x_a	x_a	x_b

The switching pattern for all the '24' regions are shown in Fig. 11.for throughout understanding the switching sequence.

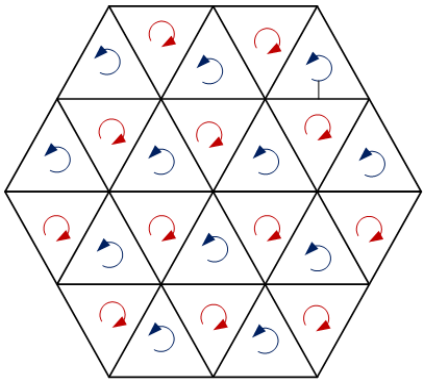

Figure 11. *Switching pulse sequence*

In odd sector vector operated are anti-clockwise in regions '1', '2' and '4'.whereas in region '3' it is clockwise. Inversely happen in even sectors.

4. Simulation Results

Simulation of 3-phase, 3-level H-bridge inverter using SVPWM technique is performed in MATLAB/SIMULINK the results are discussed. Simulation is carried out for 3 different modulation index(MI=0.42, 0.5306,0.8596) and the results are discussed here.

Fig. 11 to 14 shows simulation results for modulation index 0.42 here as shown in Fig. 12 sector will change at every sixty degree. From Fig. 13 it can be concluded that reference vector is in region '1' only. Duty ratio is varies according to α and β waveform which is observed form Fig. 14.

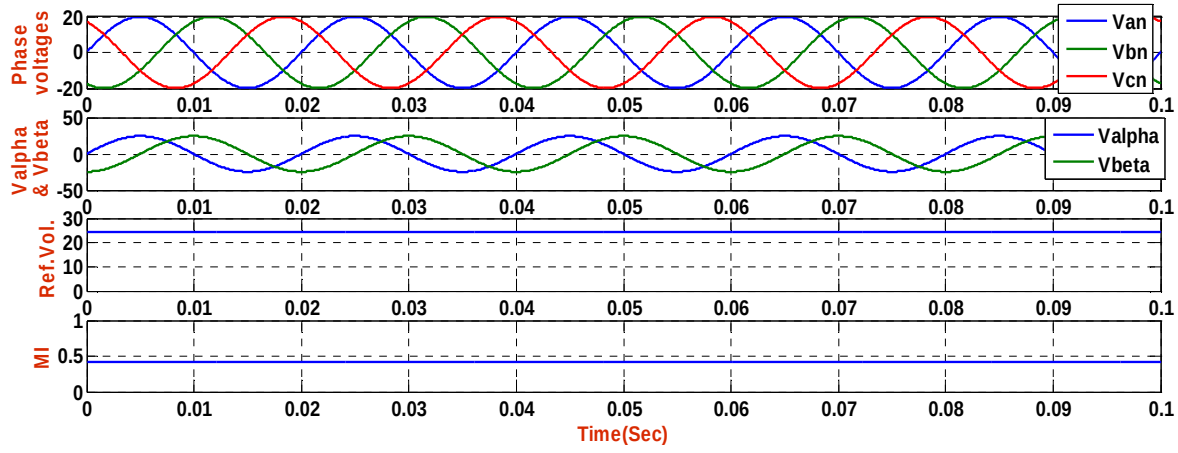

Figure 12. *(i) three phase voltages (ii)α and β component (iii) reference voltage (iv) modulation index*

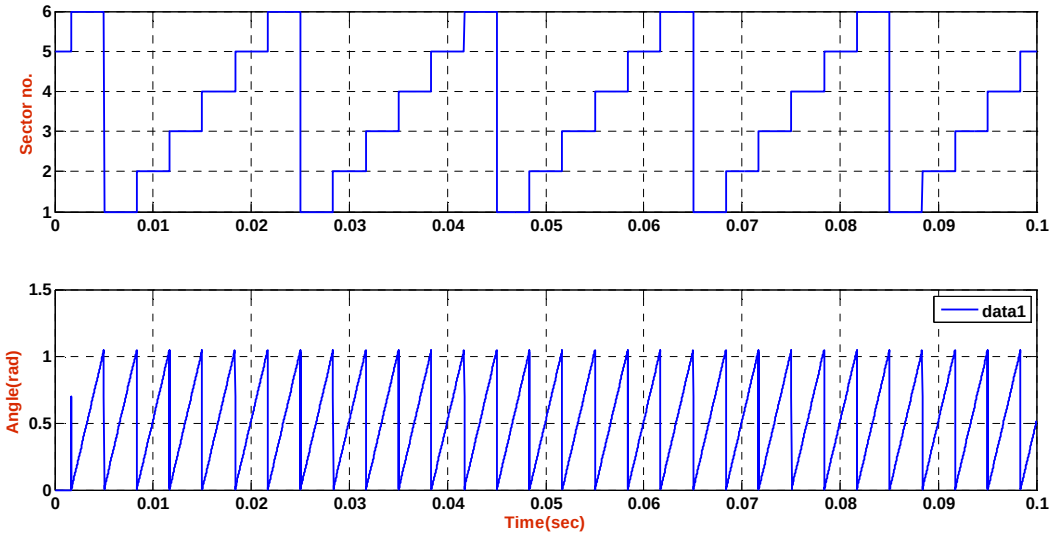

Figure 13. *(i) sector identification (ii) theta*

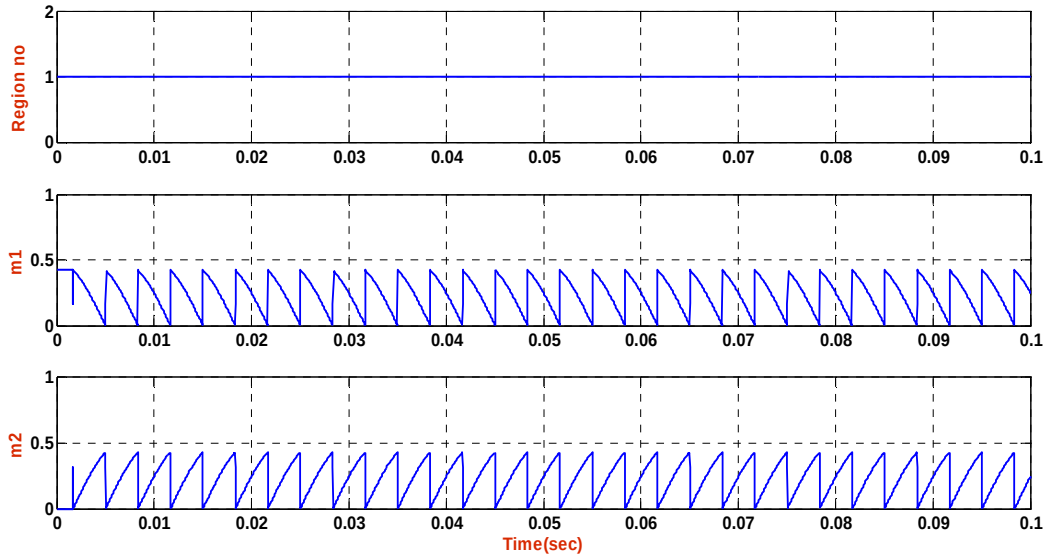

Figure 14. *(i) region identification (ii) m_1 waveform (iii) m_2 waveform*

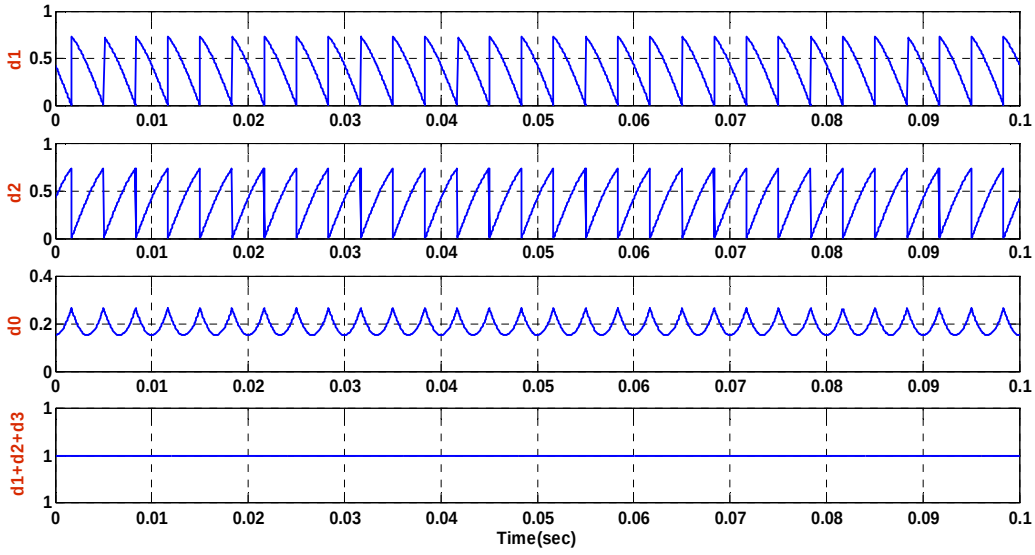

Figure 15. *Duty ratio waveform*

Below Fig.shows simulation results for modulation index 0.5306. From Fig. 16 it can be concluded that reference vector rotates in region 2,3 and 4in every sector. Duty ratio is varies according to α and β waveform which is observed from Fig. 17.

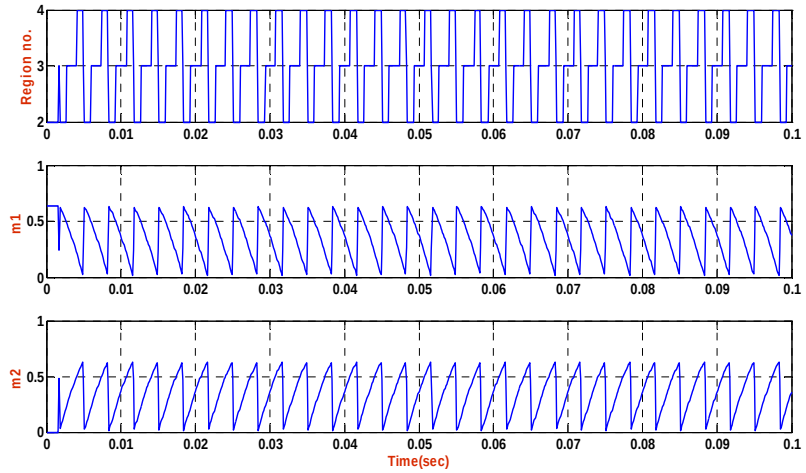

Figure 16. *(i) region identification (ii) m_1 waveform (iii) m_2 waveform*

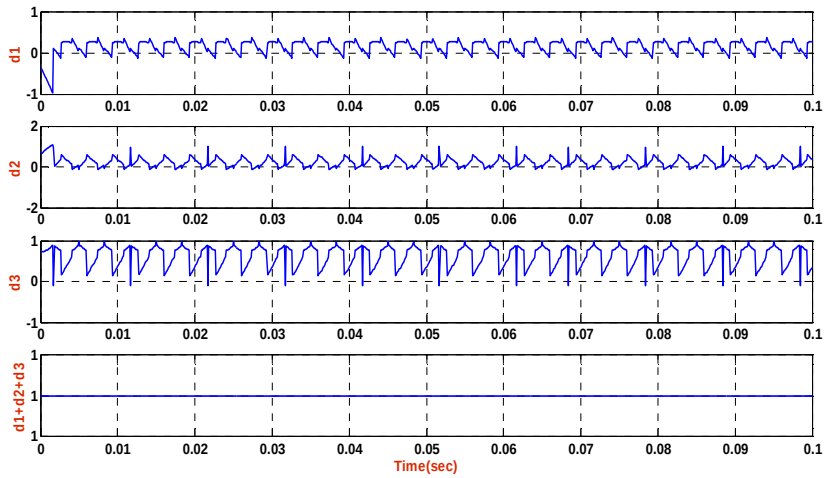

Figure 17. *Duty ratio waveform*

Below Fig. shows simulation results for modulation index 0.8596. From Fig. 17 it can be concluded that reference vector rotates in region 2 and 4 in every sector.

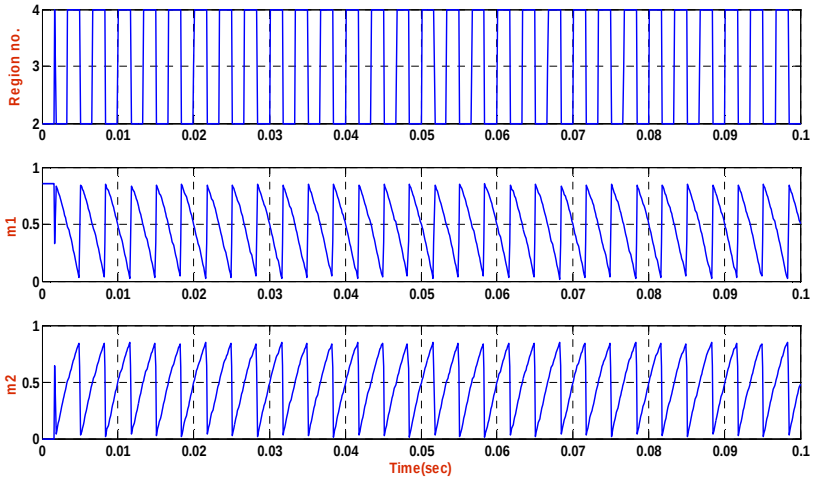

Figure 18. (i) r*egion identification (ii) m_1 waveform (iii) m_2 waveform*

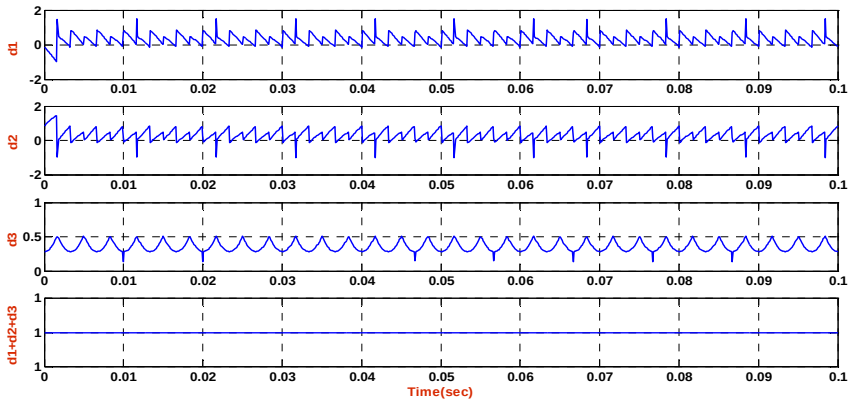

Figure 19. *Duty ratio waveform*

"In simulation from line voltages FFT analysis is performed & its fundamental value is observed for 3 different modulation index".

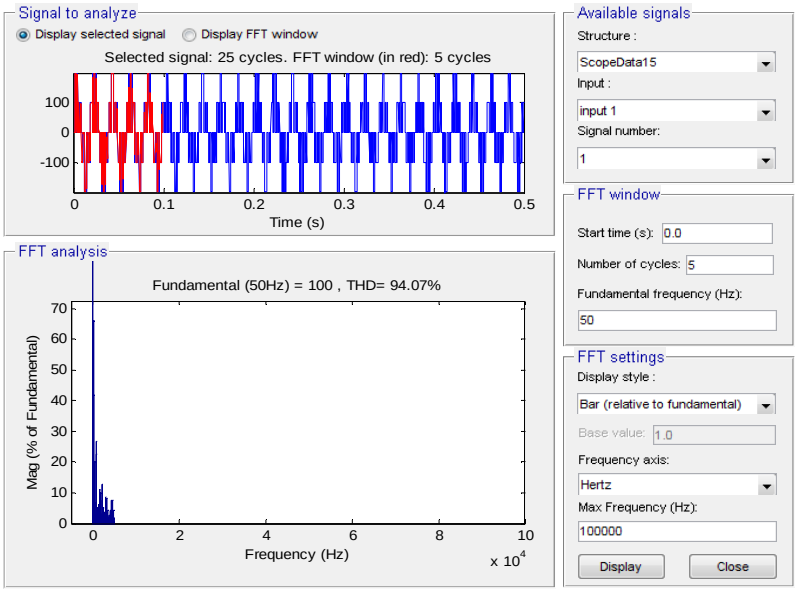

Figure 20. *FFT analysis for modulation index=0.42*

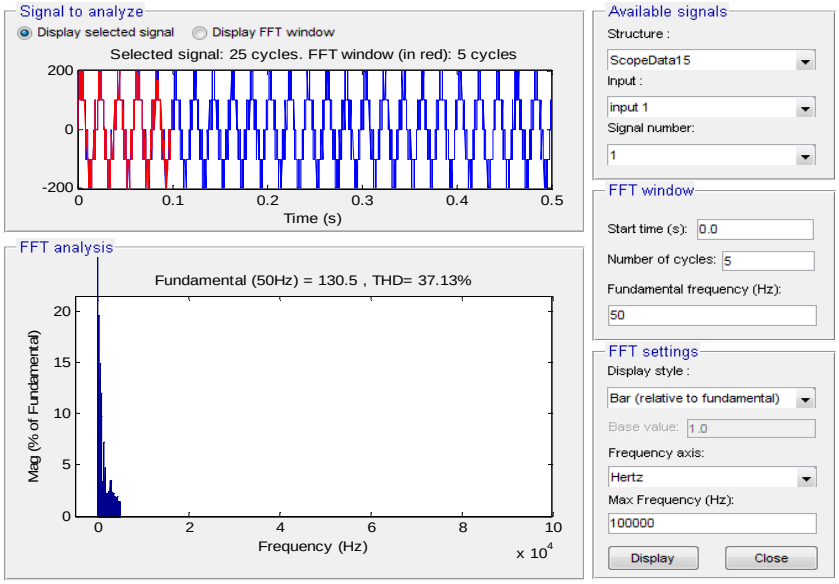

Figure 21. *FFT analysis for modulation index=0.5306*

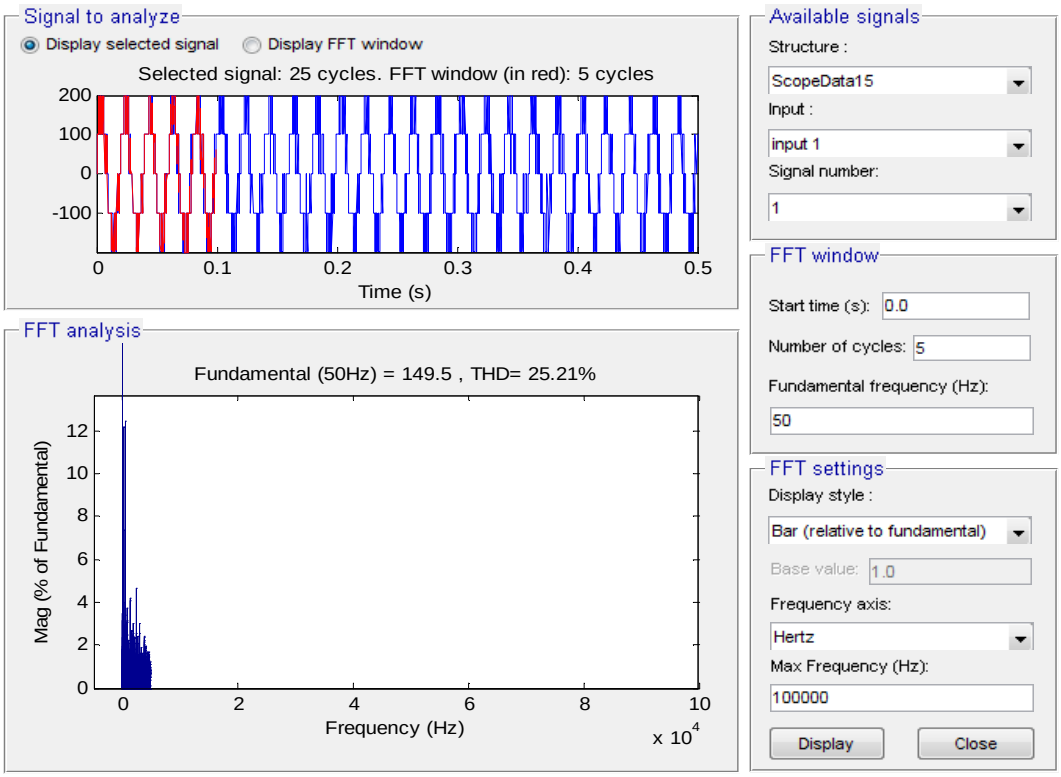

Figure 22. *FFT analysis for modulation index=0.8596*

Table 3. *line to line voltages fundamental value results*

Modulation Index	$V_{L\text{-}LFundamental}$(V)
0.44	100
0.5306	130.5
0.8596	149.5

5. Conclusion

From this paper it can be concluded that in the linear region of space vector pulse width modulation value of fundamental voltage increases according to modulation index.

Appendix A

Vector size	Vector name	Vector state	Projection on αaxis	Projection on βaxis
Small Vectors	V_{1p}	100	$\mathbf{1/2}\times\left(\frac{2}{3}V_{dc}\right)$	0
	V_{1n}	0-1-1		
	V_{2p}	110	$\frac{1}{4}\times\left(\frac{2}{3}V_{dc}\right)$	$\frac{\sqrt{3}}{4}\times\left(\frac{2}{3}V_{dc}\right)$
	V_{2n}	00-1		
	V_{3p}	010	$-\frac{1}{4}\times\left(\frac{2}{3}V_{dc}\right)$	$\frac{\sqrt{3}}{4}\times\left(\frac{2}{3}V_{dc}\right)$
	V_{3n}	-10-1		
	V_{4p}	011	$-\frac{1}{2}\times\left(\frac{2}{3}V_{dc}\right)$	0
	V_{4n}	-100		
	V_{5p}	001	$-\frac{1}{4}\times\left(\frac{2}{3}V_{dc}\right)$	$-\frac{\sqrt{3}}{4}\times\left(\frac{2}{3}V_{dc}\right)$
	V_{5n}	-1-10		
	V_{6p}	101	$\frac{1}{4}\times\left(\frac{2}{3}V_{dc}\right)$	$-\frac{\sqrt{3}}{4}\times\left(\frac{2}{3}V_{dc}\right)$
	V_{6n}	0-10		
Large Vectors	V_7	1-1-1	$\frac{3}{4}\times\left(\frac{2}{3}V_{dc}\right)$	$\frac{\sqrt{3}}{4}\times\left(\frac{2}{3}V_{dc}\right)$
	V_8	11-1	0	$\frac{\sqrt{3}}{2}\times\left(\frac{2}{3}V_{dc}\right)$
	V_9	-11-1	$-\frac{3}{4}\times\left(\frac{2}{3}V_{dc}\right)$	$\frac{\sqrt{3}}{4}\times\left(\frac{2}{3}V_{dc}\right)$
	V_{10}	-111	$-\frac{3}{4}\times\left(\frac{2}{3}V_{dc}\right)$	$-\frac{\sqrt{3}}{4}\times\left(\frac{2}{3}V_{dc}\right)$
	V_{11}	-1-11	0	$-\frac{\sqrt{3}}{2}\times\left(\frac{2}{3}V_{dc}\right)$
	V_{12}	1-11	$\frac{3}{4}\times\left(\frac{2}{3}V_{dc}\right)$	$-\frac{\sqrt{3}}{4}\times\left(\frac{2}{3}V_{dc}\right)$

Vector size	Vector name	Vector state	Projection on αaxis	Projection on βaxis
Medium Vectors	V_{13}	10-1	$\mathbf{1}\times\left(\frac{2}{3}V_{dc}\right)$	0
	V_{14}	01-1	$\frac{1}{2}\times\left(\frac{2}{3}V_{dc}\right)$	$\frac{\sqrt{3}}{2}\times\left(\frac{2}{3}V_{dc}\right)$
	V_{15}	-110	$-\frac{1}{2}\times\left(\frac{2}{3}V_{dc}\right)$	$\frac{\sqrt{3}}{2}\times\left(\frac{2}{3}V_{dc}\right)$
	V_{16}	-101	$-1\times\left(\frac{2}{3}V_{dc}\right)$	0
	V_{17}	0-11	$-\frac{1}{2}\times\left(\frac{2}{3}V_{dc}\right)$	$-\frac{\sqrt{3}}{2}\times\left(\frac{2}{3}V_{dc}\right)$
	V_{18}	1-10	$\frac{1}{2}\times\left(\frac{2}{3}V_{dc}\right)$	$-\frac{\sqrt{3}}{2}\times\left(\frac{2}{3}V_{dc}\right)$
Zero Vectors	V_{19}	000	**0**	0
		111	0	0
		-1-1-1	0	0

References

[1] S.K. Mondal, J.O.P Pinto, B.K. Bose, “A Neural-Network-Based Space Vector PWM Controller for a Three-Level Voltage-Fed Inverter Induction Motor Drive”, IEEE Trans. on I.A., Vol. 38, no. 3,May/June 2002, pp.660-669.

[2] A Multi-functional Four leg Grid Connected Compensator by R.R. Sawant and M.C.Chandorkar.

[3] D. Grahame Holmes and Thomas A. Lipo, Pulse Width Modulation For Power Converter, Principles and Practice, © 2003 The Institute of Electrical and Electronics Engineers, Inc.

[4] Shen , D., Lehn, P.W., “Fixed frequency space vector modulation control for three phase forur leg active power filters”, Electric Power Applications, IEE Proceedings, Volume 149, Issue 4, July 2002.

[5] Zhang R Prasad, V.H.Boroyevich, D. Lee F.C.. “ Three-dimensional space vector modulation for four leg voltage-source converter”, Power Electronics, IEEE Transactions on, Volume 17, May 2002

[6] A. Kocalmis, “Modelling and simulation of A Multilevel Inverter Using SVPWM”, MSc Thesis, Institute of Science, Firat University, 2005.

[7] BIMAL. K. BOSE.Modern Power Electronics and AC Drives.

[8] Rashid, M.H., 2001. Power Electronics: Circuits, Devices and Applications. NewJersey: Prentice Hall, 2001